Geophysical Research Letters

RESEARCH LETTER
10.1029/2023GL105805

Surface Cloud Warming Increases as Late Fall Arctic Sea Ice Cover Decreases

Assia Arouf[1], Hélène Chepfer[1], Jennifer E. Kay[2,3], Tristan S. L'Ecuyer[4], and Jean Lac[1]

[1]LMD/IPSL, Sorbonne Université, École Polytechnique, Institut Polytechnique de Paris, ENS, PSL Université, CNRS, Palaiseau, France, [2]CIRES, University of Colorado Boulder, Boulder, CO, USA, [3]ATOC, University of Colorado Boulder, Boulder, CO, USA, [4]Department of Atmospheric and Oceanic Sciences, University of Wisconsin-Madison, Madison, WI, USA

Key Points:

- During October, large surface cloud warming with values higher than 80 W m^{-2} occurs ∼+50% more often over open water than over sea ice
- Compared to October, November large surface cloud warming (>80 W m^{-2}) occurs even more frequently (∼+200%) over open water than over sea ice
- More frequent large surface warming caused by low-level opaque clouds occurs as open water persists later into the fall

Supporting Information:

Supporting Information may be found in the online version of this article.

Correspondence to:

A. Arouf,
aroufassia@hotmail.com

Citation:

Arouf, A., Chepfer, H., Kay, J. E., L'Ecuyer, T. S., & Lac, J. (2024). Surface cloud warming increases as late fall Arctic sea ice cover decreases. *Geophysical Research Letters*, *51*, e2023GL105805. https://doi.org/10.1029/2023GL105805

Received 3 AUG 2023
Accepted 6 DEC 2023

Author Contributions:

Conceptualization: Assia Arouf, Jennifer E. Kay
Data curation: Tristan S. L'Ecuyer
Formal analysis: Assia Arouf
Investigation: Assia Arouf, Jean Lac
Methodology: Assia Arouf, Hélène Chepfer, Jennifer E. Kay
Supervision: Hélène Chepfer
Validation: Assia Arouf
Visualization: Assia Arouf, Hélène Chepfer
Writing – original draft: Assia Arouf

Abstract During the Arctic night, clouds regulate surface energy budgets through longwave warming alone. During fall, any increase in low-level clouds will increase surface cloud warming and could potentially delay sea ice formation. While an increase in clouds due to fall sea ice loss has been observed, quantifying the surface warming is observationally challenging. Here, we use a new observational data set of surface cloud warming at instantaneous 330 m × 90 m spatial resolution. By instantaneously co-locating surface cloud warming and sea ice observations in regions where sea ice varies, we find October large surface cloud warming values (>80 W m^{-2}) are much more frequent (∼+50%) over open water than over sea ice. Notably, in November large surface cloud warming values (>80 W m^{-2}) occur more frequently (∼+200%) over open water than over sea ice. These results suggest more surface warming caused by low-level opaque clouds in the future as open water persists later into the fall.

Plain Language Summary Over the past 40 years, Arctic sea ice cover has decreased in all months of the year, but especially in late summer and early fall. Through their impact on energy budgets, clouds have the potential to increase or decrease sea ice decline. More low-level clouds over open water than over sea ice during non-summer seasons have already been observed. But quantifying their radiative effect remains challenging. Therefore, this study seeks to answer the following question: By how much late fall Arctic clouds can change surface warming in response to sea ice loss? Using cloud surface warming data at high spatio-temporal resolution, we found that large surface cloud warming values, higher than 80 W m^{-2}, occurs much more frequently over open water than over sea ice during October and November months. This suggests that Arctic clouds favor sea ice loss by delaying sea ice recovery. As the Arctic continues to warm up due to human activities, cloud surface warming will delay sea ice freeze-up later into the fall and may amplify Arctic sea ice loss.

1. Introduction

Over the past 40 years, the Arctic has warmed nearly four times faster than the global average (Rantanen et al., 2022) and also lost sea ice, especially in late summer and early fall since the satellite record began (Stroeve et al., 2012). More summer melt and a longer melt season has long been known to lead to more shortwave absorption in the Arctic ocean and greater ocean warming (Manabe & Stouffer, 1980). Warming large areas of open water can influence the adjacent ice cover, contributing to further thinning and delaying sea ice freeze-up (Stroeve et al., 2012, 2014).

Enhanced surface longwave radiation due to increased water vapor and cloudiness may accelerate sea ice melt in early spring (Huang et al., 2019) and would delay sea ice freeze-up in fall (Morrison et al., 2018), resulting in a longer melt season. Cloud-sea ice interactions is exciting to study due to their complexity but still poorly understood. Therefore, it has been the focus of several recent studies (e.g., Kay & Gettelman, 2009; Li et al., 2023; Maillard et al., 2021; Morrison et al., 2018; Monroe et al., 2021; Taylor & Monroe, 2023; Taylor et al., 2015; Yu et al., 2019). Air-sea coupling during non-summer season promotes the formation of low-level liquid clouds above open water in response to sea ice loss (Kay & Gettelman, 2009). These low-level clouds affect surface radiative fluxes and may affect sea ice formation (e.g., Taylor & Monroe, 2023). Indeed, clouds radiatively warm the surface in the longwave by trapping upward longwave earth surface radiation that would otherwise escape the earth system. Conversely, clouds radiatively cool the surface in the shortwave by reflecting solar radiation

Writing – review & editing: Hélène Chepfer, Jennifer E. Kay, Tristan S. L'Ecuyer

back to space. Low-level clouds play a stronger influence on the surface energy budget both in the longwave and the shortwave because they are usually more opaque (supercooled clouds) (Kay & Gettelman, 2009; Shupe & Intrieri, 2004; Taylor et al., 2015). During Arctic summer over the ocean, the shortwave effect dominates over the longwave effect and clouds cool the surface. In all other seasons, clouds warm the surface and may enhance sea ice loss. On average overall, Arctic clouds warm the ocean surface (e.g., Boeke & Taylor, 2016; Intrieri et al., 2002; Kay & L'Ecuyer, 2013; Schweiger & Key, 1994).

In fall, previous studies (e.g., Monroe et al., 2021; Morrison et al., 2018; Taylor & Monroe, 2023; Yu et al., 2019) found more low-level liquid clouds over open water than over sea ice. However, quantifying the surface radiative impact of these low-level clouds formed over newly open water over the entire Arctic for more than a decade is challenging. Our study investigates the following questions: (a) By how much late fall Arctic clouds can change surface longwave warming in response to sea ice cover changes? (b) How do they evolve through late fall? We use 13 years of a new observational data set of surface longwave cloud warming at instantaneous time scale and high spatial resolution (90 m cross track, 330 m along orbit track; Arouf, Chepfer, Vaillant de Guélis, Chiriaco, et al., 2022) to quantify the warming effect induced by low-level liquid clouds formed over newly open water during late fall. We found that over the last decade, low-level clouds have warmed the surface by values higher than 80 W m^{-2} in response to sea ice loss and suggest that clouds radiative warming may increase sea ice loss as the climate warms. We also document clouds between 2008 and 2020, a period with large sea ice loss and a large sea ice concentration interannual variability (Serreze & Meier, 2019).

2. Data

We use cloud data from GCM Oriented Cloud–Aerosol Lidar and Infrared Pathfinder Satellite Observations (CALIPSO) Cloud Product (CALIPSO–GOCCP v3.1.2; Chepfer et al., 2010; Cesana et al., 2012; Guzman et al., 2017; Vaillant de Guélis et al., 2017). CALIPSO data are surface type independent, that is, accurate observations over sea ice and over open water, unlike spaceborne radiometers. We use 13 years (2008–2020) of CALIPSO observations which allows having a large area where Arctic sea ice cover varies during fall. Space lidar samples vertically the atmosphere and differentiates well cloud types and each profile is classified as *Clear-sky* when no cloud is detected; *Optically Thin cloud* with optical depth <3–5 when clouds and surface echo are detected; *Opaque cloud* when clouds are detected but no surface echo is detected (Guzman et al., 2017). Opaque clouds have visible optical depth >3–5 depending on the cloud's microphysical properties (Chepfer et al., 2014) which corresponds to emissivities ranging between 0.8 and 1; *Uncertain* in all other cases (e.g., surface echo not detected and no fully attenuated altitude detected). When a cloud is detected, we can retrieve its *cloud altitude* (Vaillant de Guélis et al., 2017): the average altitude of opaque clouds $Z_{T_{Opaque}}$ which is the average altitude between cloud top altitude and the altitude where the space lidar gets completely attenuated in opaque clouds; the average altitude of thin clouds $Z_{T_{Thin}}$ which is the average altitude between cloud top altitude and cloud base altitude.

Surface longwave cloud radiative effect (LW CRE) quantifies the impact of clouds on the surface energy budget. $CRE = F^{net}_{All-sky} - F^{net}_{Cloudy-freesky}$ where the net flux is the difference between the downwelling and upwelling fluxes. We use satellite-based surface LW CRE data at two different resolutions: the new instantaneous data at 90 m cross-track and 330 m along orbit track, hereafter high spatio-temporal resolution data, and the monthly gridded data.

The new high spatio-temporal resolution surface LW CRE are from LWCRE-LIDAR Edition 1 product (Arouf, Chepfer, Vaillant de Guélis, Chiriaco, et al., 2022). This new product extends for over a decade (13 years, 2008–2020) and contains a large number of instantaneous surface LW CRE values in October ($\sim 10.10^6$ over open water, $\sim 13.10^6$ over sea ice) and in November ($\sim 5.10^6$ over open water, $\sim 17.10^6$ over sea ice). Maps of the number of profiles over each surface type and for each month are presented in Figure S3 in Supporting Information S1. These high spatio-temporal resolution data are used to study how daily sea-ice cover and surface LW CRE co-vary which is the new and main results of this paper (Figures 3 and 4).

Each lidar footprint contains either zero, for Clear-sky, a value of surface LW optically Thin CRE or a value of surface LW optically Opaque CRE. Since the space lidar cannot observe under the altitude where the lidar is fully attenuated in opaque clouds, it can miss low-level clouds under this altitude. One would think that this limitation would create a large bias in the surface LW CRE retrieval and may underestimate the surface LW CRE. However, Arctic liquid clouds that are optically opaque are usually at low levels and the space lidar attenuates most of the time in the boundary layer at altitudes lower than 3 km above the surface (Guzman et al., 2017). Uncertainties

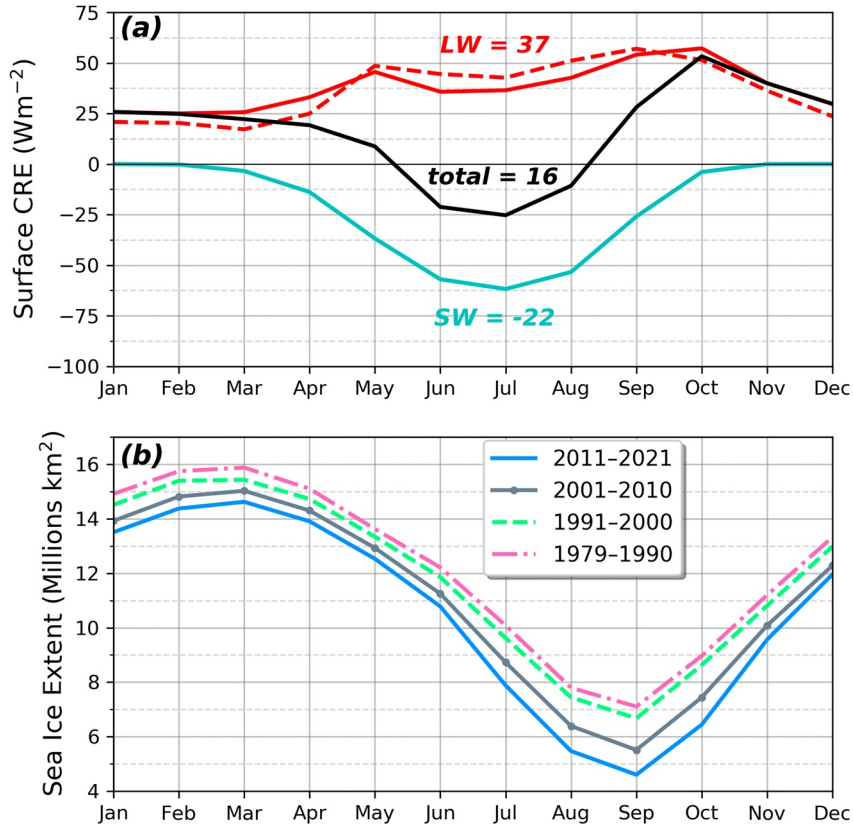

Figure 1. (a) Seasonal cycle of the surface cloud radiative effect (CRE) over Arctic oceans without northern Atlantic: longwave (LW), shortwave (SW) and total. The solid lines are from monthly gridded 2.5° × 2.5° 2BFLX product between 2007 and 2010. The dashed line is from monthly gridded 2° × 2° LWCRE–LIDAR product between 2008 and 2020. (b) Seasonal cycles of sea ice extent.

reaching ∼13W m^{-2} can be induced by the lower tropospheric temperature and humidity representations and cloud base height but would not change the overall results shown in this paper.

Monthly gridded surface CREs are used to put the context of the current study over the 2008–2011 period (Figure 1). We use monthly gridded Surface shortwave CRE data from the CloudSat 2B–FLXHR–LIDAR P1–R04 (hereafter, 2BFLX; L'Ecuyer et al., 2019) product and the monthly gridded Surface longwave CREs from both 2BFLX and the LWCRE–LIDAR Edition 1 product (Arouf, Chepfer, Vaillant de Guélis, Chiriaco, et al., 2022). The 2BFLX product at a monthly 2.5° × 2.5° resolution is currently available between August 2006 through April 2011 before CloudSat experienced a battery anomaly that limited observations to daylight only. The data set is not provided during late fall after 2011. Uncertainties in monthly mean surface longwave fluxes from 2BFLX are ∼11 W m^{-2}, owing primarily to errors in lower tropospheric temperature and humidity and uncertainty in cloud base height (Henderson et al., 2013).

Both daily and monthly sea ice concentrations are used in this study. Daily sea ice concentrations are from the National Snow and Ice Data Center's Near Real–Time SSMI EASE–Grid Daily Global Sea Ice Concentration and Snow Extent data product (NSIDC; Nolin et al., 1998). The daily sea ice data are used for establishing an area where sea ice concentration varies (Figure 2) and are also used to assign each CALIPSO footprint with a sea ice concentration value (Figures 3 and 4). Monthly sea ice extent is used between 1979 and 2021 (Fetterer et al., 2017) to set the context of this study (Figure 1).

3. Methods

We built surface masks following Morrison et al. (2018) to isolate the influence of Arctic sea ice cover variability on clouds from other cloud-controlling factors. This approach assumes that local processes affect more low-level clouds than large-scale patterns since clouds over open water and over sea ice are subject to the same large-scale atmospheric circulation regimes. We split the Arctic, defined as the area poleward 70°N, into two regions delimited

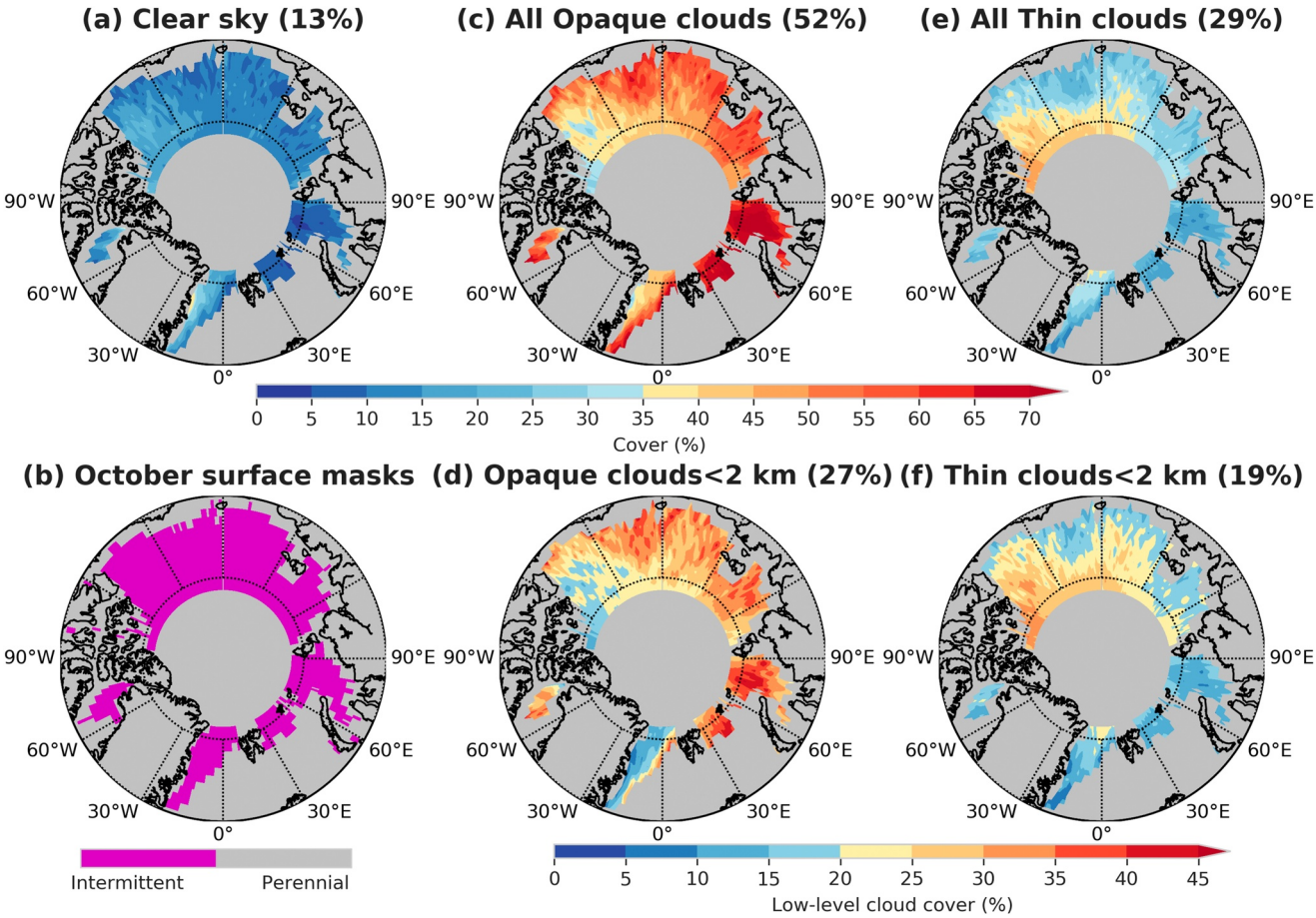

Figure 2. (a) Clear-sky cover, (b) October surface masks established between 2008 and 2020, (c) Opaque cloud cover, (d) Low-level opaque cloud cover, (e) Optically thin cloud cover, (f) Low-level optically thin cloud cover. The covers sown in the figure are built from all high spatio-temporal resolution CALIPSO–GOCCP profiles (Guzman et al., 2017) collected during October months between 2008 and 2020 period within the intermittent mask. The grid boxes with less than 100 profiles in each grid box for each October month are masked on these plots. The gray area represents the perennial mask and latitudes >82°N where CALIPSO does not collect observations. The data over the perennial mask are excluded from our study. Every other color represents the intermittent mask that isolates regions of the Arctic Ocean where the 1° × 1° daily sea ice concentration has varied between 2008 and 2020 during October months. Covers averaged over the intermittent mask are reported in parentheses. ~6% of CALIPSO–GOCCP profiles within the intermittent mask are classified as uncertain and are excluded from our study.

by two masks: the *perennial mask* and the *intermittent mask*. The perennial mask isolates regions of the Arctic where the daily sea ice concentration has not changed between 2008 and 2020 during October months. Explicitly, this mask contains grid boxes over land including coastlines, grid boxes that remain always ice-free (<15% every day between 2008 and 2020), and grid boxes that remain always ice-covered (>80% every day between 2008 and 2020). The data over the perennial mask are excluded from our study. The intermittent mask isolates regions of the Arctic Ocean where the 1° × 1° daily sea ice concentration has varied between 2008 and 2020 during October months. Specifically, the intermittent mask contains grid boxes that never remain always ice-free (<15%) nor always ice-covered (>80%). Said differently, in the intermittent mask, the daily mean sea ice concentration within a 1° × 1° grid box is not either <15% nor >80% every single day between 2008 and 2020 during October months. We built another intermittent mask for November months in the same way as for October months.

Within the intermittent mask, we split the clouds into low/high, optically opaque/thin, over open water/over sea ice using high spatio-temporal resolution cloud properties for October and November. We built *low-level opaque (optically thin) cloud cover* by dividing the number of opaque (optically thin) cloud profiles with mean altitudes $Z_{T_{Opaque}}\left(Z_{T_{Thin}}\right) < 2$ km by the total number of profiles within a 1° × 1° grid box for a given month (Figure 2).

Then we built *low-level opaque cloud cover over open water only* by dividing the number of opaque profiles with $Z_{T_{Opaque}} < 2$ km over open water (footprint sea ice cover <15%) by the total number of profiles over open water within a 1° × 1° grid box for a given month. Similarly, we built the *low-level opaque cloud cover over*

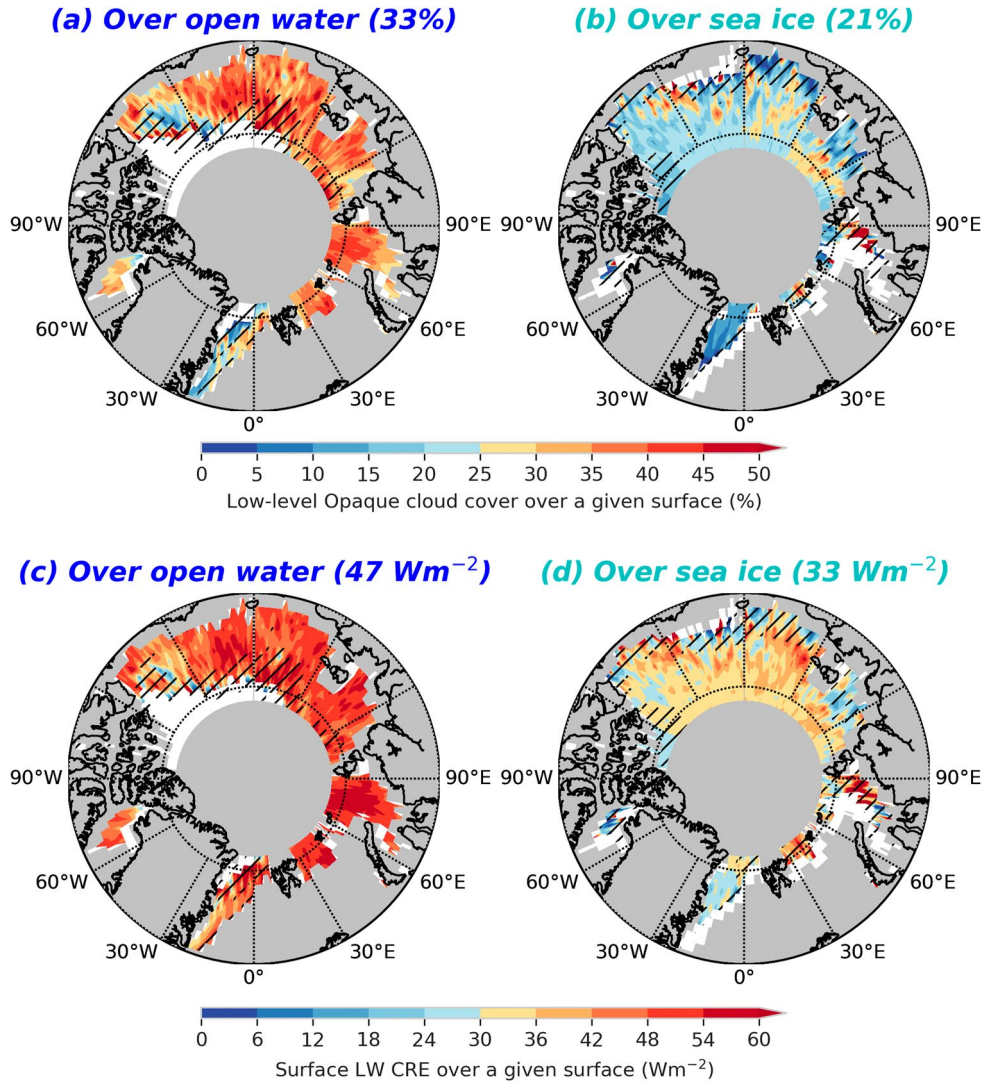

Figure 3. First line: Maps of low-level opaque cloud cover: (a) Over open water, (b) Over sea ice. Second line: Maps of surface longwave cloud warming: (c) Over open water, (d) Over sea ice. These maps are built from high spatio-temporal resolution cloud profiles and surface LW CRE values within the intermittent mask over open water only (instantaneous sea ice concentration <15%; left column) and over sea ice only (instantaneous sea ice concentration >80%; right column). The white area represents surfaces mixed with open water and sea ice (instantaneous sea ice concentration between 15% and 80%) and is excluded from our study hereafter. The grid boxes with less than 100 profiles for each October month are masked and the grid boxes with less than 5 years of data over a given surface type are dashed in the interannual means. Averages reported in parentheses include the dashed area.

sea ice only considering the profiles with footprints of sea ice cover >80%. This classification excludes profiles containing both open water and sea ice (footprint sea ice cover >15% and <80%). In the same way, we split the surface LW CRE high spatio-temporal resolution data into over open water and over sea ice and look at its distribution for opaque and thin clouds over each surface type. Similarly, we delimit the surface LW Opaque CRE high spatio-temporal resolution data caused by low-level opaque clouds (when $Z_{T_{Opaque}} < 2$ km) and by high-level opaque clouds (when $Z_{T_{Opaque}} > 2$ km) over each surface type.

4. Results

October is a particularly interesting month for investigating the observed co-variability of sea ice and cloud radiative effects (Figure 1). At this time of year, the sun is setting and cloud influence on radiative fluxes is increasingly explained by the longwave cloud warming alone. In fact, from October through February, the shortwave

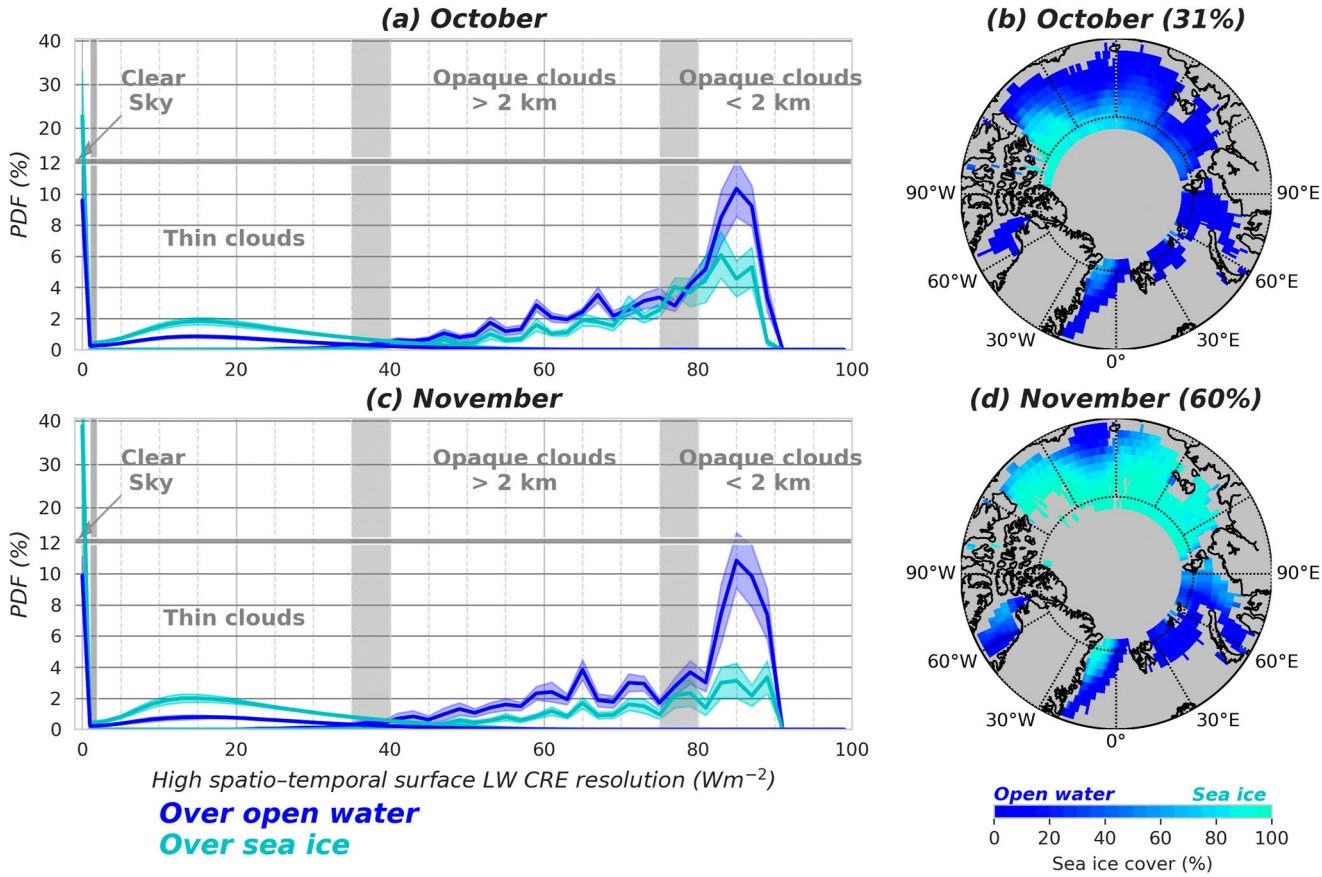

Figure 4. (a) Distribution of the high spatio-temporal resolution surface LW cloud radiative effect for October months between 2008 and 2020 within the intermittent mask over open water (instantaneous sea ice concentration <15%; blue) and over sea ice (instantaneous sea ice concentration >80%; cyan). The solid line represents the surface LW CRE interannual mean and the color-shaded regions are the interannual variance around the interannual mean. The surface LW CRE PDF is normalized by the number of all profiles over each surface type for each month. Note that the y-axe has two different graduations delimited at 12%. The gray-shaded vertical bars delimit: (i) frequency of Clear-sky profiles (surface LW CRE = 0 W m^{-2}); (ii) optically Thin clouds (optical depth < 3–5, emissivities <0.8) and have surface LW CRE between >0 and 40 W m^{-2}; (iii) high-level Opaque clouds (optical depth > 3–5, emissivities between 0.8 and 1, and $Z_{T_{Opaque}}$ > 2 km) and have surface LW CRE between 40 and 80 W m^{-2}; (iv) low-level Opaque clouds (optical depth >3–5, emissivities between 0.8 and 1, and $Z_{T_{Opaque}}$ < 2 km) and have surface LW CRE >80 W m^{-2}. (c) Same as Figure (a) but for November months over the November intermittent mask. (b, d) Maps of the monthly mean sea ice cover within the intermittent masks for October and November months respectively. Averages established over the intermittent masks are reported in parentheses.

cloud cooling is close to zero and the total cloud radiative effect is the same as the longwave cloud warming (Figure 1a). Of the months when the longwave cloud warming is the total cloud radiative effect, October has the largest Arctic sea ice loss (Figure 1b). When one compares the solid blue line (average over 2011–2021) and the dashed pink line (average over 1979–1990), October lost ~2.8 millions of km^2 of sea ice extent during this last 40 years.

To understand cloud-sea ice relationships in this interesting month, we map October high spatio-temporal resolution cloud properties within the intermittent mask which isolates regions where sea ice varies (Figure 2). October is very cloudy throughout the entire intermittent mask. Averaged over intermittent mask (Figure 2b), Clear-sky is only present ~13% of the time (Figure 2a) while clouds occur ~81% of the time (~6% of CALIPSO's profiles within the intermittent mask are classified as uncertain). We can divide this cloud cover (~81%) into optically opaque and optically thin clouds. Furthermore, more than half of October clouds are opaque (~52%), especially at lower latitudes (Figure 2c) and half of these opaque clouds have mean altitudes under 2 km (Figure 2d) resulting in low-level opaque cloud cover of ~27%. Optically thin clouds dominate at higher latitudes (>75°N), especially in the Pacific sector of the Arctic above the Canadian Archipelago (Figure 2e) which is the coldest region of the Arctic. Most thin clouds (~19% out of ~29%) also have mean altitudes under 2 km.

Low-level opaque clouds are the dominant cloud type during October months within the intermittent mask (Figure 2d; ~27% of CALIPSO's profiles) and warm the surface more than the other clouds. Therefore, we

focus on these clouds. We examine clouds over open water (sea ice concentration <15%) and over sea ice (sea ice concentration >80%) (Figure 3). Maps show there are more low-level opaque clouds over open water than over sea ice in almost all locations. When averaged over the intermittent mask, there are ∼12% more low-level opaque clouds over open water than over sea ice. This low-level opaque clouds cover difference over open water and over sea ice is responsible for larger surface cloud warming over open water than over sea ice at all latitudes. Specifically, surface cloud warming over open water (47 W m^{-2}) is larger than surface cloud warming over sea ice (33 W m^{-2}) when averaged over the entire intermittent mask (Figures 3c and 3d).

Analyzing the distribution of high spatio-temporal resolution surface longwave cloud warming over open water and over sea ice (Figure 4a) shows the largest values occur more over open water than they do over sea ice. Specifically, large values (>80 W m^{-2}) are much more frequent (∼+ 50%) over open water than over sea ice and are caused by low-level opaque clouds. Figure S4 in Supporting Information S1 supports the fact that we have more large surface cloud warming over open water compared to over sea ice at all latitudes due to the low-level clouds' response to sea ice loss (Kay & Gettelman, 2009; Morrison et al., 2018) and not due to differences in cloud temperature along latitudes or profile sampling along latitude. For optically thin clouds, even though they are numerous at averaged altitudes lower than 2 km, they warm less the surface with high spatio-temporal resolution surface longwave cloud warming up to 40W m^{-2}. Clear-sky profiles occur much more frequently over sea ice than over open water (22% vs. 9%) and are responsible for the low values of the averaged surface LW CRE over sea ice (maps Figure 3d).

Comparing October with November, a month with less open water in the observational record (Figures 4b and 4d) shows that like October, November also has more low-level opaque clouds over open water than over sea ice within the November intermittent mask (Figures S1 and S2 in Supporting Information S1). The low-level opaque cloud cover differences over sea ice and over open water are 12% in October and 24% in November. Therefore, even though November has a lot more sea ice within the intermittent mask (59% in November vs. 31% in October), the low-level opaque cloud cover differences seen in October persist into November. Consistent with these low-level opaque cloud cover differences, there are also more very large high spatio-temporal resolution surface longwave cloud warming (values > 80 W m^{-2}) over open water than over sea ice. But, unlike October, the occurrence frequency difference is even larger in November. In November, large high spatio-temporal resolution surface longwave cloud warming (values > 80 W m^{-2}) occurs ∼+200% more frequently over open water than over sea ice.

5. Discussion and Conclusions

This manuscript addresses an important climate question: How much do clouds contribute to warming of the Arctic Ocean as sea ice begins to re-form each late fall? This study shows for the first time the observed link between the daily sea-ice cover where sea-ice varies and the value of the surface longwave cloud warming at high spatio-temporal resolution derived from space lidar, using 13 years of data over the entire Arctic region. Our study shows that over the last decade, low-level clouds have warmed the surface by values higher than 80 W m^{-2} in response to sea ice loss and suggests that cloud radiative warming may increase sea ice loss as the climate warms.

Specifically, we show that large surface cloud warming values (>80 W m^{-2}) occur more than ∼+50% of the time more often over open water than over sea ice during late fall. This occurrence difference is consistent with previous work (e.g., Morrison et al., 2018) that found more low-level clouds over open water than over sea ice but they did not quantify their radiative effect on the surface radiative budget and this is the novelty of our study. Our results suggest that cloud surface warming could lengthen the melt season by delaying sea ice freeze-up. We show that low-level opaque clouds formed over newly open water warm the surface during late fall. These low-level opaque clouds are dominant in regions where sea ice varies (intermittent mask) and are more numerous over open water than over sea ice. Using high spatio-temporal resolution surface warming data, we found that large values of surface longwave cloud warming occur ∼+50% more often over open water than over sea ice during October months. During November compared to October, we found an even higher increase in the occurrence of large surface longwave cloud warming over open water than over sea ice. Thus, low-level opaque clouds warm the surface ∼+200% more often over open water than over sea ice during November. The difference in large surface LW CRE values occurrence over open water and over sea ice (larger over open water) is mostly due to the difference in frequency of low-level opaque clouds which are more frequent over open water than over sea ice (Figure

S5 in Supporting Information S1). The low-level opaque cloud optical depth difference over open water and over sea ice would play a secondary role as all clouds classified as opaque in this study have a large emissivity (0.8–1).

Uncertainties in the high spatio-temporal resolution surface longwave cloud warming values would not change the overall results drawn in this study. Specifically, uncertainties in the high spatio-temporal resolution surface longwave cloud warming data set might be induced by the space lidar not seeing the opaque cloud base as discussed in the method section. The altitude of low opaque clouds $\left(Z_{T_{Opaque}}\right)$ would be even lower if the cloud base is documented better. Therefore, the values of the high spatio-temporal resolution surface longwave cloud warming would be larger. The space lidar missing the cloud base height results in less occurrence of large values of surface longwave cloud warming. Said differently, large surface longwave cloud warming would occur even more frequently than +50% over open water compared to over sea ice during October months if the space lidar documents better cloud base height and would emphasize more the fact that large surface longwave cloud warming occurs more frequently over open water than over sea ice. ∼6% of CALIPSO profiles are classified as uncertain and are excluded from our study but their percentage remains small to change drastically our results. Adding to this, ∼25% of all CALIPSO profiles occur over mixed surface types during October months and are excluded from our study when we split CALIPSO's profiles into over open water and over sea ice.

Our results suggest even more large surface longwave cloud warming as the Arctic goes ice-free. Indeed, during the last two decades, sea ice has been subject to more melt and longer melt seasons with quite a lot of variability (Serreze & Meier, 2019), that is, early melt season onset and a delay in the freeze-up season leaving more open water later into the fall. As the Arctic warms, the melt season is expected to lengthen further (Stroeve et al., 2014) leading to more open water in late fall. Future November may look more like present October and future December may look like present November with a huge increase in the occurrence of large surface longwave cloud warming over open water than over sea ice. Said in other words, more open water extent as the Arctic goes sea ice-free in the future (Kim et al., 2023) combined with ocean-atmosphere coupling during non-summer seasons, will promote low-level cloud formation (Kay & Gettelman, 2009; Palm et al., 2010; Sato et al., 2012) leading to more frequent large surface cloud warming values (>80 W m^{-2}; Figure 4).

To sum up, our study helps to improve our understanding of cloud influence on surface energy budget during late fall as Arctic sea ice retreats, thanks to a new high spatio-temporal resolution (instantaneous data at 330 m × 90 m) surface longwave cloud warming data set. We quantify the surface longwave warming induced by low-level clouds as sea ice retreats in late fall and suggest that surface longwave cloud warming would help to lengthen the melt season by potentially delaying sea ice freeze-up.

Data Availability Statement

The LWCRE–LIDAR–Ed1 is available for the 2008–2020 time period for the monthly 2° × 2° gridded data set (Arouf, Chepfer, Vaillant de Guélis, Guzman, et al., 2022), and for the data set along orbit track (Arouf et al., 2023). The 2BFLX monthly 2.5° × 2.5° data set for the 2007–2010 time period is described in Henderson et al. (2013). The NSIDC sea ice extent data set is available between 1979 and 2021 (Fetterer et al., 2017).

Acknowledgments
We are grateful to Airbus for funding AA. We thank NASA/CNES for the CALIPSO level-1 data and the Mesocentre ESPRI/IPSL for the computational resources. We recognize the support of CNES for the development of the CALIPSO–GOCCP product. Contributions of JEK and TSL were funded by NASA CloudSat/CALIPSO Science Team Grant 80NSSC20K0135.

References

Arouf, A., Chepfer, H., Vaillant de Guélis, T., Chiriaco, M., Shupe, M. D., Guzman, R., et al. (2022). The surface longwave cloud radiative effect derived from space lidar observations. *Atmospheric Measurement Techniques*, *15*(12), 3893–3923. https://doi.org/10.5194/amt-15-3893-2022

Arouf, A., Chepfer, H., Vaillant de Guélis, T., Guzman, R., Feofilov, A., & Raberanto, P. (2022). Longwave cloud radiative effect derived from space lidar observations at the surface and toa—Edition 1: Monthly gridded product [Dataset]. IPSL. https://doi.org/10.14768/70d5f4b5-e740-4d4c-b1ec-f6459f7e5563

Arouf, A., Chepfer, H., Vaillant de Guélis, T., Guzman, R., Feofilov, A., & Raberanto, P. (2023). Longwave cloud radiative effect derived from space lidar observations at the surface and toa—Edition 1: Along orbit track (2008–2020) [Dataset]. IPSL. https://doi.org/10.14768/d4de28c3-0912-4244-8c2b-6fe259eb863c

Boeke, R. C., & Taylor, P. C. (2016). Evaluation of the Arctic surface radiation budget in CMIP5 models. *Journal of Geophysical Research: Atmospheres*, *121*(14), 8525–8548. https://doi.org/10.1002/2016JD025099

Cesana, G., Kay, J. E., Chepfer, H., English, J. M., & de Boer, G. (2012). Ubiquitous low-level liquid-containing Arctic clouds: New observations and climate model constraints from CALIPSO-GOCCP. *Geophysical Research Letters*, *39*(20), L20804. https://doi.org/10.1029/2012GL053385

Chepfer, H., Bony, S., Winker, D., Cesana, G., Dufresne, J. L., Minnis, P., et al. (2010). The GCM-oriented CALIPSO cloud product (CALIPSO-GOCCP). *Journal of Geophysical Research*, *115*(D4), D00H16. https://doi.org/10.1029/2009JD012251

Chepfer, H., Noel, V., Winker, D., & Chiriaco, M. (2014). Where and when will we observe cloud changes due to climate warming? *Geophysical Research Letters*, *41*(23), 8387–8395. https://doi.org/10.1002/2014GL061792

Fetterer, F., Knowles, K., Meier, W. N., Savoie, M., & Windnagel, A. K. (2017). Sea ice index, version 3 [Dataset]. National Snow and Ice Data Center. https://doi.org/10.7265/N5K072F8

Guzman, R., Chepfer, H., Noel, V., Vaillant de Guélis, T., Kay, J. E., Raberanto, P., et al. (2017). Direct atmosphere opacity observations from CALIPSO provide new constraints on cloud-radiation interactions. *Journal of Geophysical Research: Atmospheres*, *122*(2), 1066–1085. https://doi.org/10.1002/2016JD025946

Henderson, D. S., L'Ecuyer, T., Stephens, G., Partain, P., & Sekiguchi, M. (2013). A multisensor perspective on the radiative impacts of clouds and aerosols [Dataset]. Cloudsat, *52*, 853–871. https://doi.org/10.1175/JAMC-D-12-025.1

Huang, Y., Dong, X., Bailey, D. A., Holland, M. M., Xi, B., DuVivier, A. K., et al. (2019). Thicker clouds and accelerated Arctic sea ice decline: The atmosphere-sea ice interactions in spring. *Geophysical Research Letters*, *46*(12), 6980–6989. https://doi.org/10.1029/2019GL082791

Intrieri, J. M., Fairall, C. W., Shupe, M. D., Persson, P. O. G., Andreas, E. L., Guest, P. S., & Moritz, R. E. (2002). An annual cycle of Arctic surface cloud forcing at SHEBA. *Journal of Geophysical Research*, *107*(C10), SHE13-1–SHE13-14. https://doi.org/10.1029/2000JC000439

Kay, J. E., & Gettelman, A. (2009). Cloud influence on and response to seasonal Arctic sea ice loss. *Journal of Geophysical Research*, *114*(D18), D18204. https://doi.org/10.1029/2009JD011773

Kay, J. E., & L'Ecuyer, T. (2013). Observational constraints on Arctic Ocean clouds and radiative fluxes during the early 21st century. *Journal of Geophysical Research: Atmospheres*, *118*(13), 7219–7236. https://doi.org/10.1002/jgrd.50489

Kim, Y.-H., Min, S.-K., Gillett, N. P., Notz, D., & Malinina, E. (2023). Observationally-constrained projections of an ice-free Arctic even under a low emission scenario. *Nature Communications*, *14*(1), 3139. https://doi.org/10.1038/s41467-023-38511-8

L'Ecuyer, T. S., Hang, Y., Matus, A. V., & Wang, Z. (2019). Reassessing the effect of cloud type on earth's energy balance in the age of active spaceborne observations. Part I: Top of atmosphere and surface. *Journal of Climate*, *32*(19), 6197–6217. https://doi.org/10.1175/JCLI-D-18-0753.1

Li, X., Mace, G. G., Strong, C., & Krueger, S. K. (2023). Wintertime cooling of the Arctic TOA by low-level clouds. *Geophysical Research Letters*, *50*(17), e2023GL104869. https://doi.org/10.1029/2023GL104869

Maillard, J., Ravetta, F., Raut, J.-C., Mariage, V., & Pelon, J. (2021). Characterisation and surface radiative impact of Arctic low clouds from the IAOOS field experiment. *Atmospheric Chemistry and Physics*, *21*(5), 4079–4101. https://doi.org/10.5194/acp-21-4079-2021

Manabe, S., & Stouffer, R. J. (1980). Sensitivity of a global climate model to an increase of CO_2 concentration in the atmosphere. *Journal of Geophysical Research*, *85*(C10), 5529–5554. https://doi.org/10.1029/JC085iC10p05529

Monroe, E. E., Taylor, P. C., & Boisvert, L. N. (2021). Arctic cloud response to a perturbation in sea ice concentration: The north water polynya. *Journal of Geophysical Research: Atmospheres*, *126*(16), e2020JD034409. https://doi.org/10.1029/2020JD034409

Morrison, A. L., Kay, J. E., Chepfer, H., Guzman, R., & Yettella, V. (2018). Isolating the liquid cloud response to recent Arctic sea ice variability using spaceborne lidar observations. *Journal of Geophysical Research: Atmospheres*, *123*(1), 473–490. https://doi.org/10.1002/2017JD027248

Nolin, A., Armstrong, R., & Maslanik, J. (1998). Near-real-time SSM/I-SSMIS EASE-grid daily global ice concentration and snow extent, version 4. NASA national snow and ice data center distributed. *Active Archive Center*, *10*. https://doi.org/10.5067/VF7QO90IHZ99

Palm, S. P., Strey, S. T., Spinhirne, J., & Markus, T. (2010). Influence of Arctic sea ice extent on polar cloud fraction and vertical structure and implications for regional climate. *Journal of Geophysical Research*, *115*(D21), D21209. https://doi.org/10.1029/2010JD013900

Rantanen, M., Karpechko, A. Y., Lipponen, A., Nordling, K., Hyvärinen, O., Ruosteenoja, K., et al. (2022). The Arctic has warmed nearly four times faster than the globe since 1979. *Communications Earth & Environment*, *3*(1), 1–10. https://doi.org/10.1038/s43247-022-00498-3

Sato, K., Inoue, J., Kodama, Y.-M., & Overland, J. E. (2012). Impact of Arctic sea-ice retreat on the recent change in cloud-base height during autumn. *Geophysical Research Letters*, *39*(10), L10503. https://doi.org/10.1029/2012GL051850

Schweiger, A. J., & Key, J. R. (1994). Arctic Ocean radiative fluxes and cloud forcing estimated from the ISCCP C2 cloud dataset, 1983–1990. *Journal of Applied Meteorology and Climatology*, *33*(8), 948–963. https://doi.org/10.1175/1520-0450(1994)033⟨0948:AORFAC⟩2.0.CO;2

Serreze, M. C., & Meier, W. N. (2019). The Arctic's sea ice cover: Trends, variability, predictability, and comparisons to the Antarctic. *Annals of the New York Academy of Sciences*, *1436*(1), 36–53. https://doi.org/10.1111/nyas.13856

Shupe, M. D., & Intrieri, J. M. (2004). Cloud radiative forcing of the Arctic surface: The influence of cloud properties, surface albedo, and solar zenith angle. *Journal of Climate*, *17*(3), 616–628. https://doi.org/10.1175/1520-0442(2004)017⟨0616:CRFOTA⟩2.0.CO;2

Stroeve, J. C., Markus, T., Boisvert, L., Miller, J., & Barrett, A. (2014). Changes in Arctic melt season and implications for sea ice loss. *Geophysical Research Letters*, *41*(4), 1216–1225. https://doi.org/10.1002/2013GL058951

Stroeve, J. C., Serreze, M. C., Holland, M. M., Kay, J. E., Malanik, J., & Barrett, A. P. (2012). The Arctic's rapidly shrinking sea ice cover: A research synthesis. *Climatic Change*, *110*(3–4), 1005–1027. https://doi.org/10.1007/s10584-011-0101-1

Taylor, P. C., Kato, S., Xu, K.-M., & Cai, M. (2015). Covariance between Arctic sea ice and clouds within atmospheric state regimes at the satellite footprint level. *Journal of Geophysical Research: Atmospheres*, *120*(24), 12656–12678. https://doi.org/10.1002/2015JD023520

Taylor, P. C., & Monroe, E. (2023). Isolating the surface type influence on Arctic low-clouds. *Journal of Geophysical Research: Atmospheres*, *128*(16), e2022JD038098. https://doi.org/10.1029/2022JD038098

Vaillant de Guélis, T., Chepfer, H., Noel, V., Guzman, R., Dubuisson, P., Winker, D. M., & Kato, S. (2017). The link between outgoing longwave radiation and the altitude at which a spaceborne lidar beam is fully attenuated. *Atmospheric Measurement Techniques*, *10*(12), 4659–4685. https://doi.org/10.5194/amt-10-4659-2017

Yu, Y., Taylor, P. C., & Cai, M. (2019). Seasonal variations of Arctic low-level clouds and its linkage to sea ice seasonal variations. *Journal of Geophysical Research: Atmospheres*, *124*(22), 12206–12226. https://doi.org/10.1029/2019JD031014